ARMY RESEARCH LABORATORY

Wave Propagation in Second-order Nonlinear Piezoelectric Media

by David A. Hopkins and George A. Gazonas

ARL-TR-5766 **September 2011**

NOTICES

Disclaimers

The findings in this report are not to be construed as an official Department of the Army position unless so designated by other authorized documents.

Citation of manufacturer's or trade names does not constitute an official endorsement or approval of the use thereof.

Destroy this report when it is no longer needed. Do not return it to the originator.

Army Research Laboratory

Aberdeen Proving Ground, MD 21005-5066

ARL-TR-5766 **September 2011**

Wave Propagation in Second-order Nonlinear Piezoelectric Media

David A. Hopkins and George A. Gazonas

Weapons and Materials Research Directorate, ARL

REPORT DOCUMENTATION PAGE

Form Approved
OMB No. 0704-0188

1. REPORT DATE *(DD-MM-YYYY)*	2. REPORT TYPE	3. DATES COVERED (From - To)
September 2011	Final	January 2010-December 2010

4. TITLE AND SUBTITLE
Wave Propagation in Second-order Nonlinear Piezoelectric Media

5a. CONTRACT NUMBER

5b. GRANT NUMBER

5c. PROGRAM ELEMENT NUMBER

6. AUTHOR(S)
David A. Hopkins
George A. Gazonas

5d. PROJECT NUMBER
AH42

5e. TASK NUMBER

5f. WORK UNIT NUMBER

7. PERFORMING ORGANIZATION NAME(S) AND ADDRESS(ES)
U.S. Army Research Laboratory
ATTN: RDRL-WMM-B
Aberdeen Proving Ground, MD 21005-5066

8. PERFORMING ORGANIZATION REPORT NUMBER
ARL-TR-5766

9. SPONSORING/MONITORING AGENCY NAME(S) AND ADDRESS(ES)

10. SPONSOR/MONITOR'S ACRONYM(S)

11. SPONSOR/MONITOR'S REPORT NUMBER(S)

12. DISTRIBUTION/AVAILABILITY STATEMENT
Approved for public release; distribution is unlimited.

13. SUPPLEMENTARY NOTES
david.a.hopkins.civ@mail.mil

14. ABSTRACT

Computational results for the response of piezoelectric materials to various excitations are presented. The governing equations are based on a second-order theory of piezoelectricity, which is specialized for the 6mm crystal class. The equations are formulated in a Lagrangian reference configuration. These equations represent the fully coupled nonlinear multiphysics response. Numerical solutions of these equations are first verified using analytical solutions for wave propagation in linear piezoelectric media. The effects of the nonlinear coupling introduced by higher order elastic, dielectric, and piezoelectric coupling coefficients are then examined.

15. SUBJECT TERMS
piezoelectricity, constitutive laws, multiphysics

16. SECURITY CLASSIFICATION OF:			17. LIMITATION OF ABSTRACT	18. NUMBER OF PAGES	19a. NAME OF RESPONSIBLE PERSON
a. REPORT	b. ABSTRACT	c. THIS PAGE			David A Hopkins
Unclassified	Unclassified	Unclassified	UU	42	19b. TELEPHONE NUMBER (*Include area code*) 410-306-0764

Contents

List of Figures

List of Tables

INTENTIONALLY LEFT BLANK.

1. Introduction

In 1880 Pierre and Jacques Curie experimentally demonstrated the direct piezoelectricity effect in which a mechanical load generates an electric charge. In 1881 Lippman (*1*), based on thermodynamic considerations, postulated the inverse effect, where an electric field generates a mechanical response. His prediction was subsequently confirmed by the Curies. Voigt presented the first general thermodynamic theory of piezoelectricity during the 1890–1894 time frame (*2*). Since then, various theories of linear piezoelectricity have arisen based upon assumptions concerning both deformation and the material constitutive response. The majority of these theories begin with linear elasticity and the assumption of a symmetric stress tensor (*3*). Some researchers have tried to reformulate the governing equations in terms of a Cosserat continuum (*4*). Additional simplifying assumptions are subsequently used to develop equations relevant for plates, shells, and beams (*5–7*).

The behavior of piezoelectric materials in non-structural applications has been investigated extensively. However, these investigations almost exclusively employ linear constitutive relations. For example, piezoelectricity is undergoing a resurgence in both fundamental research and technical applications (*8–12*). However, investigations in the nonlinear basic theory for piezoelectricity have been limited. Nelson (*13*), Toupin (*14*), and Tiersten (*15, 16*) studied the nonlinear theory of dielectrics. Norwood et al. (*17*) and Kulkami and Hanagud (*18*) used a Neo-Hookean constitutive relation to model the response of piezoelectric ceramics. Pai et al. (*19*) considered the dependence of the piezoelectric strain parameters upon the strain in formulating a plate theory of piezoelectric laminates. Joshi (*20*) considered the nonlinear constitutive relations for piezoelectric materials, where a concise expression was given. Tiersten (*21*) investigated the nonlinear problems of thin plates subjected to large driving voltages. Recently, Patel et al. used finite element techniques to solve a particular form of the nonlinear piezoelectric equations with a nonlinear stress-strain relationship but linear electrostatics (*22*). However, they assume that the effects of the nonlinear constitutive can be neglected and only include nonlinear strain effects. Based on the theory of invariants, from invariant polynomial constitutive relations, Yang and Batra (*23*) investigated the second-order theory for piezoelectric materials with symmetry class 6mm and class mm2. Feng et al. (*24*), using results from Kiral and Eringen (*25*), developed the relations for symmetry classes 6mm and 3m including both nonlinear stress-strain and electrostatic constitutive relations.

In this report, we present the Feng et al. (*24*) equations in a form suitable for numerical solution. These equations are then specialized for one dimensional (1-D) use. Numerical solutions are verified by comparison with exact solutions of the linear piezoelectric equations obtained using Laplace transform techniques. Finally, the response of the full nonlinear equations to both step pressure and step voltage boundary conditions are examined.

2. Finite Deformation Piezoelectricity

The aforementioned theories are typically obtained by formulating the equations of piezoelectricity starting with principles from continuum mechanics. This approach provides a general formulation with a clearer understanding of the restrictions on deformation and material constitutive response imposed upon the resulting governing equations. The equations of motion, in the current (Eulerian) configuration, can be written as (*26*)

$$T_{kl,k} + \rho b_l = \rho \ddot{u}_l \quad , \tag{1}$$

where ρ is the material density, b_l is the body force, $\ddot{u}_l$ is the particle acceleration, and T_{kl} is the total stress. Lowercase Latin subscripts indicate quantities that refer to the current configuration while uppercase Latin subscripts indicate quantities that refer to the reference configuration with subscripts ranging from 1–3. Partial differentiation is denoted by a comma before the index. In equation 1, symmetry of the stress tensor is not required although we include it in the following. Additionally, there are no assumptions concerning the form of the constitutive relationships. Including mechanical and electromagnetic forces, the total stress, T_{kl}, can be written as (*23*)

$$T_{kl} = T^C_{kl} + \epsilon_0 \hat{E}_k \hat{E}_l - \frac{1}{2}\epsilon_0 \hat{E}_m \hat{E}_m \delta_{kl} \quad . \tag{2}$$

T^C is the Cauchy stress and the remaining terms are the Maxwell stress expressed in the current configuration (*27*), where ϵ_0 is the electric permittivity of free space, $\hat{E}$ is the electric field, and δ_{kl} is the Kronecker delta.

The equations of motion in the reference (Lagrangian) configuration are obtained from equation 1. The equivalence of the divergence in different reference frames is given by

$$(G_{kl})_{,k} = \frac{1}{J}(J F^{-1}_{Kk} G_{kl})_{,K} \quad , \tag{3}$$

where G is an arbitrary second rank tensor, $F_{kK} \equiv x_{k,K}$ is the deformation gradient, and

$J = det(F)$. Cauchy stress, T^C_{kl}, is written in terms of the second Piola-Kirchoff stress, T_{KL} as

$$T^C_{kl} = \frac{1}{J} x_{k,K} T_{KL} x_{l,L} = \frac{1}{J} F_{kK} T_{KL} F_{lL} \quad . \tag{4}$$

The electric field and electric displacement transformations are given by (*28*)

$$\hat{E}_k \;\; = \;\; X_{K,k} E_K = F^{-1}_{Kk} E_K \tag{5}$$

$$\hat{D}_k \;\; = \;\; \frac{1}{J} x_{k,K} D_K = \frac{1}{J} F_{kK} D_K \tag{6}$$

where E and D are the electric field and the electric displacement in the reference configuration, respectively, and $\hat{E}$ and $\hat{D}$ are the fields in the current configuration.

The appropriate transformation for the polarization, $\hat{P}_k$, has been the subject of debate (*29, 30*). Several commonly used transformation are shown in table 1. Yang and Batra (*31*) used a set of transformations that are very different from the traditionally accepted forms, including the transformation for the electric field. Dorfmann and Ogden (*29*) used a form that is more commonly accepted. Their rationale for the form of the transformation for the polarization is that the form can be selected so as to simplify mathematical manipulation of the equations. Clayton (*30*) selected a form of the transformation for the polarization based on this premise. As shown by Lax and Nelson (*28*), the forms of the transformations for all the field variables, including polarization, are not arbitrary. The appropriate transformation for the polarization is determined by consideration of conservation of charge, which leads to

$$\hat{P}_k \;\; = \;\; \frac{1}{J} x_{k,K} \Pi_K = \frac{1}{J} F_{kK} \Pi_K \tag{7}$$

where $\hat{P}$ and Π are the polarization in the current and reference configurations, respectively.

Table 1. Transformation relations.

Author	**Electric Displacement**	**Electric Field**	**Polarization**
Yang/Batra (*31*)	$D_A = JF^{-1}_{Aa}\hat{D}_a$	$E_A = JF^{-1}_{Aa}\hat{E}_a$	$\Pi_A = JF^{-1}_{Aa}\hat{P}_a$
Dorfmann/Ogden (*29*)	$D_A = JF^{-1}_{Aa}\hat{D}_a$	$E_A = F_{aA}\hat{E}_a$	$\Pi_A = JF^{-1}_{Aa}\hat{P}_a$
Clayton (*30*)	$D_A = JF^{-1}_{Aa}\hat{D}_a$	$E_A = F_{aA}\hat{E}_a$	$\Pi_A = F_{aA}\hat{P}_a$
Lax/Nelson (*28*)	$D_A = JF^{-1}_{Aa}\hat{D}_a$	$E_A = F_{aA}\hat{E}_a$	$\Pi_A = JF^{-1}_{Aa}\hat{P}_a$

Using the relations $F^{-1}_{Kk} \equiv X_{K,k}$, $J\rho = \rho_0$, where ρ_0 is the density referred to the reference configuration with equations 3–7, the equation of motion in the Lagrangrian frame can finally be written

$$(T_{KL}x_{l,L})_{,K} + (JF^{-1}_{Kk}(\epsilon_0 F^{-1}_{Mk}F^{-1}_{Nl} - \frac{1}{2}\epsilon_0 F^{-1}_{Mm}F^{-1}_{Nm}\delta_{kl})E_M E_N)_{,K} + \rho_0 b_l = \rho_0 \ddot{u}_l \quad . \tag{8}$$

Equation 8 represents the balance of forces acting on a volume of material. There are 12 unknowns, 6 stress components, 3 electric field components, and 3 displacements. The additional equations required for a consistent formulation are obtained from the governing equations relating the electric field components and the piezoelectric constitutive laws.

The governing equations relating the electric field components are obtained by starting with Gauss's law with no free charges,

$$(\hat{D}_k)_{,k} = 0 \quad , \tag{9}$$

where $\hat{D}$ is the electric displacement. Then, using the constitutive relationship $\hat{D}_k = \epsilon_0 \hat{E}_k + \hat{P}_k$, equation 9 becomes

$$(\epsilon_0 J F^{-1}_{Kk}F^{-1}_{Mk}E_M + \Pi_K)_{,K} = 0 \quad . \tag{10}$$

The Euler-Piola-Jacobi identity (*32*), $(JF^{-1}_{Kk})_{,K} = 0$, is used to simplify equation 10 to

$$(\Pi_K)_{,K} + \epsilon_0 J F^{-1}_{Kk}(F^{-1}_{Mk}E_M)_{,K} = 0 \quad . \tag{11}$$

Equations 8 and 11 are the equations of motion and Gauss's law in the reference configuration. Closed-form solutions to the full equations given by equations 8 and 11 do not appear feasible.

A standard approach for solving these equations is the use of numerical methods. For instance, the Galerkin method is often applied in finite element methods. Another approach is to reduce the equations to one dimension and seek exact solutions. As shown below, we will illustrate both of the approaches. Accordingly, we first express the governing equations, 8 and 11, in their corresponding weak forms. Then, we reduce the equations to their 1-D representations. Finally, we can also obtain solutions to these equations in one dimension using Laplace transform techniques, assuming that the displacements are infinitesimal and that the piezoelectric constitutive relations are linear. We then can compare solutions to the full equations expressed in the weak form with the 1-D exact solutions.

3. Weak Form Expressions

The weak form of the governing equations is obtained using Galerkin's method (*33*). Applying this technique to equations 8 and 11 leads to (*34*)

$$
\begin{aligned}
&-\int_{\Omega_0}(T_{KL}x_{l,L}+(JF^{-1}_{Kk}(\epsilon_0F^{-1}_{Mk}F^{-1}_{Nl}-\frac{1}{2}\epsilon_0F^{-1}_{Mm}F^{-1}_{Nm}\delta_{kl})E_ME_N))v_{l,K}d\Omega_0+\int_{\Omega_0}\rho_0b_lv_ld\Omega_0\\
&-\int_{\Omega_0}\rho_0\ddot{u}_lv_ld\Omega_0+\int_{\Gamma_0}(T_{KL}x_{l,L}+(JF^{-1}_{Kk}(\epsilon_0F^{-1}_{Mk}F^{-1}_{Nl}-\frac{1}{2}\epsilon_0F^{-1}_{Mm}F^{-1}_{Nm}\delta_{kl})E_ME_N))n_Kv_ld\Gamma_0\\
&-\int_{\Omega_0}(\Pi_K+\epsilon_0JF^{-1}_{Kk}(F^{-1}_{Mk}E_M))\Phi_{,K}d\Omega_0+\int_{\Gamma_0}(\Pi_K+\epsilon_0JF^{-1}_{Kk}(F^{-1}_{Mk}E_M))n_K\Phi d\Gamma_0=0
\end{aligned}
\tag{12}
$$

where v_l and Φ are arbitrary displacement and scalar electric potential test functions, respectively, Ω_0 is the domain of the reference configuration with boundary Γ_0, and n_K is the outward normal on the boundary. Assuming the response is magnetostatic, the electric field, E, can be expressed as the gradient of Φ

$$E=-\nabla\Phi \quad . \tag{13}$$

The variational statement can therefore be written

$$
\begin{aligned}
&-\int_{\Omega_0}(T_{KL}x_{l,L}+(JF^{-1}_{Kk}(\epsilon_0F^{-1}_{Mk}F^{-1}_{Nl}-\frac{1}{2}\epsilon_0F^{-1}_{Mm}F^{-1}_{Nm}\delta_{kl})\Phi_{,M}\Phi_{,N}))v_{l,K}d\Omega_0+\int_{\Omega_0}\rho_0b_lv_ld\Omega_0\\
&-\int_{\Omega_0}\rho_0\ddot{u}_lv_ld\Omega_0+\int_{\Gamma_0}(T_{KL}x_{l,L}+(JF^{-1}_{Kk}(\epsilon_0F^{-1}_{Mk}F^{-1}_{Nl}-\frac{1}{2}\epsilon_0F^{-1}_{Mm}F^{-1}_{Nm}\delta_{kl})\Phi_{,M}\Phi_{,N}))n_Kv_ld\Gamma_0\\
&-\int_{\Omega_0}(\Pi_K-\epsilon_0JF^{-1}_{Kk}(F^{-1}_{Mk}\Phi_{,M}))\Phi_{,K}d\Omega_0+\int_{\Gamma_0}(\Pi_K-\epsilon_0JF^{-1}_{Kk}(F^{-1}_{Mk}\Phi_{,M}))n_K\Phi d\Gamma_0=0 \quad .
\end{aligned}
\tag{14}
$$

For small electric fields, equation 14 reduces to

$$
\begin{aligned}
-\int_{\Omega_0}T_{KL}x_{l,L}v_{l,K}d\Omega_0+\int_{\Omega_0}\rho_0b_lv_ld\Omega_0-\int_{\Omega_0}\rho_0\ddot{u}_lv_ld\Omega_0-\int_{\Omega_0}\Pi_K\Phi_{,K}d\Omega_0&\\
+\int_{\Gamma_0}T_{KL}x_{l,L}n_Kv_ld\Gamma_0+\int_{\Gamma_0}\Pi_Kn_K\Phi d\Gamma_0 &= 0 \quad .
\end{aligned}
\tag{15}
$$

The solution of these equations is obtained by minimizing each equation with respect to each test function.

To complete the equations, T_{KL} and Π_K are related to the strains and the electric field by appropriate constitutive relations. These relations are obtained from

$$T_{KL} = \frac{\partial \Sigma}{\partial \Gamma_{KL}} \tag{16}$$

$$\Pi_K = \frac{\partial \Sigma}{\partial E_K} \quad . \tag{17}$$

where Σ is the free energy density function. Expressions for Σ are lengthy. Feng et al. (*35*), and Kiral and Eringen (*25*) provide explicit expressions. In one dimension, these expressions reduce to

$$T = c^E \Gamma - eE + \frac{1}{2} C \Gamma^2 - \frac{1}{2} Q E^2 - g \Gamma E \quad , \tag{18}$$

$$\Pi = e\Gamma + \epsilon E + \frac{1}{2} g \Gamma^2 + \frac{1}{2} \eta E^2 + Q \Gamma E \tag{19}$$

where c^E is the second-order elastic stiffness coefficient, e is the piezoelectric coupling coefficient, ϵ is the dielectric permittivity, C is the third-order elastic coefficient, Q is electrostrictive coefficient, g is the third-order piezoelectric coupling coefficient, and η is the third-order dielectric permittivity. Γ is the finite strain measure. The components of Γ are given by

$$\Gamma_{IJ} = \frac{1}{2} \left(\frac{\partial u_I}{\partial X_J} + \frac{\partial u_J}{\partial X_I} + \frac{\partial u_K}{\partial X_I} \frac{\partial u_K}{\partial X_J} \right) \quad , \tag{20}$$

which in one dimension reduces to

$$\Gamma = \frac{\partial u}{\partial Z} + \frac{1}{2} \left(\frac{\partial u}{\partial Z} \right)^2 \quad . \tag{21}$$

Consequently, with deformation restricted to one dimension and neglecting the Maxwell stress and body force terms, the final weak form expression is given by

$$\int_0^l (-T(1 + u_{,Z}) v_{,Z} - \Pi \Phi_{,Z} + \rho_0 \ddot{u} v) dX \quad + T x_{,Z} \, v \mid_0^l + \Pi \Phi \mid_0^l \quad = 0 \quad . \tag{22}$$

Numerical solutions of equation 22 were obtained using the COMSOL Multiphysics analysis software (*36*). The generalized α method was employed as the time dependent solver. As this solver is only A-stable, it exhibits spurious high frequency ringing when subjected to a step loading (*37*). To address this issue, artificial Rayleigh damping was incorporated by adding an

additional weak term in the form (*38*)

$$d_R = -\int \nu_R c^E \frac{\partial v}{\partial x}[\frac{\partial}{\partial t}\frac{\partial u}{\partial x}]dX \tag{23}$$

to the left-hand side of equation 22, where ν_R is an adjustable parameter used to minimize the oscillations in the solution.

4. Laplace Transform Solutions

Solutions of equation 22 can be verified by comparison with solutions to the strong form of the equations that are either exact solutions or solutions obtained by a different numerical technique. When considering the deformations in equations 8 and 11 to be infinitesimal and the electric fields to be small, and neglecting body forces, it is possible to obtain solutions that can be considered exact for all practical purposes using Laplace transform techniques. With the assumptions given, equation 8 reduces to the standard wave equation

$$\rho\frac{d^2u}{dt^2} = \frac{d\sigma_x}{dx} \tag{24}$$

In equation 24 and the following, we express all equations in the more commonly found partial derivative forms rather than indicial notation. The 1-D constitutive equations for a linear piezoelectric material can be written as (*39*)

$$\sigma_x = c^D\frac{du}{dx} - hD_x, \tag{25}$$

$$E_x = -h\frac{du}{dx} + D_x/\varepsilon, \tag{26}$$

where σ_x is the stress in newtons/m^2, c^D is Young's modulus (at constant electric displacement) in newtons/m^2, u is the particle displacement in meters, D_x is the electric flux density in the x-direction in coul/m^2, ε is the permittivity in farads/m, h is a piezoelectric constant in V/m, and E_x is the x-component of the electric field in V/m (N/coul). This form of the constitutive relationship is more amenable to analytic solutions than other equivalent forms of the piezoelectric constitutive relationships. However, the use of different constitutive relations requires determination of the appropriate transformations relating the constitutive coefficients. In equations 25 and 26, $c^D = c^E + eh$ and $h = e/\epsilon$. These transformations are discussed in appendix B.

Substitution of equation 25 into equation 24 gives,

$$\frac{d^2u}{dt^2} = \frac{c^D}{\rho}\frac{d^2u}{dx^2} - h\rho\frac{dD_x}{dx}. \tag{27}$$

Assuming plane wave propagation, and that there is no free charge inside the piezoelectric medium, Gauss's Law, given by equation 9, reduces to

$$\frac{dD_x}{dx} = 0, \tag{28}$$

Consequently, equation 27 again reduces to the 1-D wave equation for isotropic elastic (nonpiezoelectric) media and can be written as

$$\frac{d^2u}{dt^2} = \frac{c^D}{\rho}\frac{d^2u}{dx^2}. \tag{29}$$

4.1 1-D Plane Wave Solutions

In this section, we find solutions to equation 29 with linear constitutive equations given by equations 25 and 26 for the boundary conditions listed in table 2. Figure 1 depicts the location and orientation of the boundary conditions. The solutions are obtained by assuming the displacements u in the piezoelectric medium can be expressed as D'Alembert functions, e.g.,

$$u(x,t) = F_2(t - x/c) + F_1(t + x/c) \tag{30}$$

where $c = \sqrt{c^D/\rho}$.

Table 2. Boundary conditions.

Location	**Step Voltage**	**Resonance**	**Step Pressure**
$x = 0$	$\phi = H(t), T = 0$	$\phi = 0, T = sin(\omega t)$	$\phi = 0, T = T_0 H(t)$
$x = l$	$\phi = 0, T = 0$	$\phi = 0, T = 0$	$\phi = 0, u = 0$

Using the fact that $\mathcal{L}[f(t-\tau)H(t-\tau)] = e^{-s\tau}F(s) \qquad t > 0$, Laplace transform of equation 30 gives

$$\mathcal{L}[u(x,t)] = \bar{u}(x,s) = e^{\frac{-sx}{c}}\bar{F}_2(s) + e^{\frac{sx}{c}}\bar{F}_1(s) \quad . \tag{31}$$

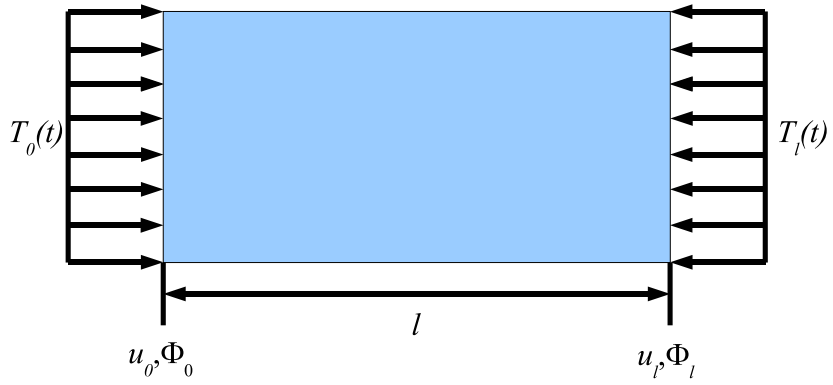

Figure 1. 1-D boundary value problem.

Substitution of the spatial derivative of equation 30 into equation 25 yields,

$$\sigma_x + hD_x = \frac{c^D}{c}[-F_2'(t - x/c) + F_1'(t + x/c)] \quad . \tag{32}$$

To find the potential across a plate of thickness, l, integrate equation 26:

$$V(t) = \int_0^l E_x(x,t)dx, \tag{33}$$

or

$$V(t) = -h[u(l) - u(0)] + lD_x(t)/\varepsilon, \tag{34}$$

where the quantity $u(l) - u(0)$ represents the relative motion of the plate surfaces. Letting $\sigma_x = \sigma(x,t)$, $D_x(t) = D(t)$ and taking the Laplace transform of equation 32 gives

$$\bar{\sigma}(x,s) + h\bar{D} = \frac{c^D}{c}[-se^{\frac{-sx}{c}}\bar{F}_2(s) + se^{\frac{sx}{c}}\bar{F}_1(s)]. \tag{35}$$

Laplace transform of the stress-free boundary at 0, $\bar{\sigma}(0,s) = 0$ results in

$$h\bar{D} = \frac{c^D}{c}[-s\bar{F}_2(s) + s\bar{F}_1(s)] \tag{36}$$

and of the stress-free boundary at l, $\bar{\sigma}(l,s) = 0$ results in

$$h\bar{D} = \frac{c^D}{c}[-se^{\frac{-sl}{c}}\bar{F}_2(s) + se^{\frac{sl}{c}}\bar{F}_1(s)]. \tag{37}$$

Simultaneous solution of equations 36 and 37 gives

$$\bar{F}_2(s) = -e^{\frac{sl}{c}}\bar{F}_1(s). \tag{38}$$

Taking the Laplace transform of equation 34 and substitution of equation 31 gives

$$\bar{V}(s) = -h[e^{\frac{-sl}{c}}\bar{F}_2(s) + e^{\frac{sl}{c}}\bar{F}_1(s) - \bar{F}_2(s) - \bar{F}_1(s)] + l\bar{D}/\varepsilon, \tag{39}$$

or

$$\bar{V}(s) = h[\bar{F}_2(s)(1 - e^{\frac{-sl}{c}}) + \bar{F}_1(s)(1 - e^{\frac{sl}{c}})] + l\bar{D}/\varepsilon. \tag{40}$$

Substitution of equation 38 into equation 36 yields

$$F_2(s) = \frac{-ch\bar{D}e^{\frac{sl}{c}}}{c^D s(1 + e^{\frac{sl}{c}})}, \tag{41}$$

or

$$F_1(s) = \frac{ch\bar{D}}{c^D s(1 + e^{\frac{sl}{c}})} \tag{42}$$

Substitution of equations 41 and 42 into equation 40 results in an expression for the Laplace transformed potential:

$$\bar{V}(s) = \bar{D}\left(\frac{l}{\epsilon} - \frac{2ch^2\tanh\left(\frac{sl}{2c}\right)}{Ms}\right) \tag{43}$$

For a step voltage input applied to a stress free plate, $V(t) = V_0H(t)$ and $\bar{V}(s) = V_0/s$. Also $I(t) = dQ(t)/dt = dD(t)/dt$, so $\bar{I} = s\bar{Q} = s\bar{D}$. The Laplace transformed current can be written as

$$\bar{I}(s) = s\bar{Q}(s) = s\bar{D}(s) = \frac{sc^D\epsilon V_0}{c^D sl - 2ch^2\epsilon\tanh\left(\frac{ls}{2c}\right)} \tag{44}$$

Also, from equation 35, we have on rearrangement

$$\bar{\sigma}(x,s) = \frac{c^D}{c}[-se^{\frac{-sx}{c}}\bar{F}_2(s) + se^{\frac{sx}{c}}\bar{F}_1(s)] - h\bar{D}. \tag{45}$$

Substitution of equations 41 through 43 into equation 45 results in the Laplace transformed stresses:

$$\bar{\sigma}(x,s) = \frac{2hc^D\epsilon\sinh\left(\frac{s(l-x)}{2c}\right)\sinh\left(\frac{sx}{2c}\right)V_0}{2ch^2\epsilon\sinh\left(\frac{ls}{2c}\right) - c^D sl\cosh\left(\frac{ls}{2c}\right)}. \tag{46}$$

The time domain solutions are found by numerical inversion of the Laplace transform using the Dubner-Abate-Crump (DAC) algorithm described by Crump (*40*). The effects of Gibbs'

phenomena are mitigated using the so-called Lanczos σ-factors with 2048 terms and a tolerance equal to 10^{-4} (*43*). Following similar procedures, the Laplace transformed stresses for the response to a sinusoidal voltage and a step pressure are given by

$$\bar{\sigma}(x,s) = \frac{(2s\omega hc^D \epsilon V_0 sinh(\frac{s(l-x)}{(2c)})sinh(\frac{sx}{(2c)}))}{(s^2+\omega^2)(-lc^D scosh(\frac{ls}{(2c)})) + (2ch^2 \epsilon sinh(\frac{ls}{(2c)}))} \tag{47}$$

and

$$\bar{\sigma}(x,s) = \frac{(lc^D scosh(\frac{sx}{c}) - ch^2 \epsilon sinh(\frac{ls}{c}))P_0}{lc^D s^2 cosh(\frac{ls}{c}) - ch^2 s\epsilon sinh(\frac{ls}{c})} \tag{48}$$

4.2 Plane Waves in a Free-free Bi-material Plate

Finally, we can also obtain solutions for a bi-material plate (figure 2) using Laplace transforms. Assuming that the displacements in materials 1 and 2 are given by u_1 and u_2, respectively, we can write

$$\begin{aligned} u_1(x,t) &= F_2(t - x/c_1) + F_1(t + x/c_1) \\ u_2(x,t) &= F_4(t - x/c_2) + F_3(t + x/c_2). \end{aligned} \tag{49}$$

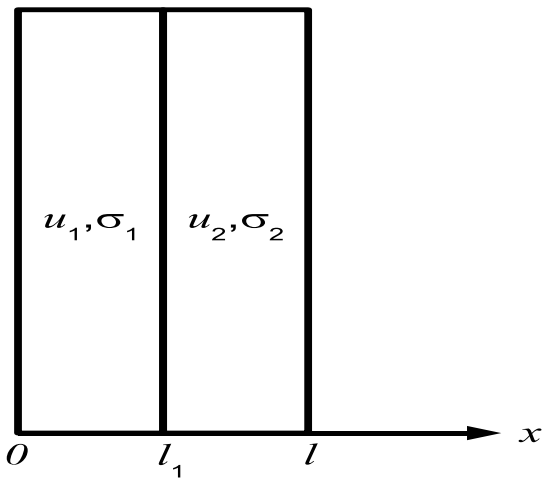

Figure 2. Two-layer boundary value problem.

Substitution of the spatial derivatives of equation 49 into equation 25 yields,

$$\begin{aligned}\sigma_1(x,t) &= c_1^D \tfrac{du_1}{dx} - h_1 D_1 = \tfrac{c_1^D}{c_1}[-F_2'(t-x/c_1] + F_1'(t+x/c_1] - h_1 D_1 \\ \sigma_2(x,t) &= c_2^D \tfrac{du_2}{dx} - h_2 D_2 = \tfrac{c_2^D}{c_2}[-F_4'(t-x/c_2] + F_3'(t+x/c_2] - h_2 D_2.\end{aligned} \tag{50}$$

Taking Laplace transforms of the stress and displacement boundary conditions with reference to the coordinate system shown in figure 2, together with the assumption that there are no free charges in the dielectrics, i.e., $\left(\vec{D}_1 - \vec{D}_2\right) \cdot \hat{n} = 0$, and $D_1(s) = D_2(s) = D(s)$, permits determination of the unknown functions F_1, F_2, F_3, and F_4, in equations 49 via

$$\begin{aligned}\bar{\sigma}_1(l_1,s) &= \bar{\sigma}_2(l_1,s) \\ \bar{u}_1(l_1,s) &= \bar{u}_2(l_1,s) \\ \bar{\sigma}_1(0,s) &= 0 \\ \bar{\sigma}_2(l,s) &= 0,\end{aligned} \tag{51}$$

or

$$\begin{aligned}&\tfrac{c_1^D}{c_1}[-se^{\frac{-l_1}{c_1}}\bar{F}_2(s) + se^{\frac{l_1}{c_1}}\bar{F}_1(s)] - h_1\bar{D}(s) = \tfrac{c_2^D}{c_2}[-se^{\frac{-l_1}{c_2}}\bar{F}_4(s) + se^{\frac{l_1}{c_2}}\bar{F}_3(s)] - h_2\bar{D}(s) \\ &e^{\frac{-l_1}{c_1}}\bar{F}_2(s) + e^{\frac{l_1}{c_1}}\bar{F}_1(s) = e^{\frac{-l_1}{c_2}}\bar{F}_4(s) + e^{\frac{l_1}{c_2}}\bar{F}_3(s) \\ &\tfrac{c_1^D}{c_1}[-s\bar{F}_2(s) + s\bar{F}_1(s)] - h_1\bar{D}(s) = 0 \\ &\tfrac{c_2^D}{c_2}[-se^{\frac{-l}{c_2}}\bar{F}_4(s) + se^{\frac{l}{c_2}}\bar{F}_3(s)] - h_2\bar{D}(s) = 0\ .\end{aligned} \tag{52}$$

Since the piezoelectric layers are arranged in series, the total potential can be written as that for capacitors in series via $V(t) = V_1(t) + V_2(t)$, where,

$$\begin{aligned}V_1(t) &= \int_0^{l_1} E_x(x,t)dx \\ V_2(t) &= \int_{l_1}^{l} E_x(x,t)dx\ .\end{aligned} \tag{53}$$

Substitution of equation 26 into equations 53, integrating and then Laplace transforming the result, allows determination of the unknown time-varying function $D(t)$, which appears in

equations 50 as was done in equation 44. Prescribing a voltage boundary condition $V(t)$ allows determination of the voltages via

$$\begin{aligned}\bar{V}_1(s) &= -h_1[e^{\frac{-l_1}{c_1}}\bar{F}_2(s) + e^{\frac{l_1}{c_1}}\bar{F}_1(s) - \bar{F}_2(s) - \bar{F}_1(s)] + l_1\bar{D}(s)/\varepsilon_1 \\ \bar{V}_2(s) &= -h_2[e^{\frac{-l}{c_2}}\bar{F}_4(s) + e^{\frac{l}{c_2}}\bar{F}_3(s) - e^{\frac{-l_1}{c_2}}\bar{F}_4(s) - e^{\frac{-l_1}{c_2}}\bar{F}_3(s)] + l\bar{D}(s)/\varepsilon_2 - l_1\bar{D}(s)/\varepsilon_2 \ .\end{aligned} \tag{54}$$

Finally, the expressions for F_1, F_2, F_3, F_4 and $D(s)$ can be used to obtain the solutions for $\sigma_1(x,s)$ and $\sigma_2(x,s)$. These solutions are provided in appendix A, equations A-1 and A-2.

5. Material Properties

From equations 18 and 19, it is seen that eight material properties are required for the nonlinear constitutive law. Three of these coefficients are the typical elastic moduli, a; piezoelectric coupling term, e; and the dielectric constant, ϵ. Extensive literature can be found documenting these material properties. For example, values for alpha-quartz at low temperatures have even been measured (*41*), although the authors do note that even in the case of quartz, inconsistent values for the elastic and piezoelectric constants are often reported.

The remaining five coefficients are less readily available with even more uncertainty concerning the accuracy of reported values. Davison and Graham (*42*) present third-order elastic coefficients for several materials. However, they only have third-order piezoelectric constants for lithium niobate, and quartz. These constants can also be estimated, with appropriate assumptions, using pressure derivatives as discussed by Clayton (*30*), if such data are available. While this approach could be used, for the purposes of this report, it is sufficient to recognize that when the response is restricted to one dimension that the distinction between different crystal classes is not relevant. Accordingly, the coefficients of X-cut quartz for which these properties have been experimentally determined have been used. The properties are shown in table 3. The linear values are also shown. Both quartz and lead zirconate titanate (PZT) were used in verifying the numerical implementation by comparing the predicted response with exact solutions to the linear equations.

Table 3. Material properties for quartz and PZT.

Material Name	**Quartz**(*42*)			**PZT**(*36*)
	Present	**D&G**	Value	
Elastic stiffness (GPa)	c^E	C_{33}^E	86.736	115.41
Piezoelectric coupling (C/m^2)	e	e_{33}	0.171	15.08
Dielectric constant (ε^0)	ε	ε_{33}^η	4.40	663.2
Third-order elastic (GPa)	C	C_{333}^E	-300.0	
Third-order piezoelectric (ε^0 m/V)	g	$\frac{1}{2}e_{ijklm}$	-1.31	
Electrostrictive (ε^0 F/m)	Q	f_{333}	-4.40	
Third-order dielectric (F/V)	η	ε_{333}^η	$O(-3.5 \times 10^{-17})$	
Density (kg/m^3)	ρ		2651	7500

6. Results

The solution of equation 22 was verified by comparing with exact solutions obtained by using a modified DAC algorithm for numerically inverting the Laplace transform (*43*) of the linear piezoelectric equations for a simple disk of unit cross-sectional area and unit thickness.

Chen and Davison presented results for the nonlinear response of a piezoelectric material (*44*). They present results where the material properties remains elastic and nonconducting. Consequently, the nonlinearity they discuss is one of finite deformation, not material nonlinearity.

In this report, we present exact transient solutions (in the sense of a Laplace transform solution) for linear elastic piezoelectric media. Yang presents results for a similar problem but restricted to harmonic response (*45*). Redwood also solves for the transient response using Laplace transform techniques, though the discussion is mostly limited to qualitative results (*46*).

The poling direction was aligned with the axial direction of the disk. In the first verification, a short circuit solution was obtained for a step voltage with the boundary conditions listed in table 2. The voltage drop was 1 V across the thickness, t. In the second verification, an oscillatory pressure boundary condition was applied. The frequency, ω, was chosen to be close to the axial resonance frequency of the disk.

Figures 3 and 4 show COMSOL numerical results to a step voltage for PZT-4 and quartz, respectively. Figure 3 shows the stress response at the location $x = L/2$ for PZT-4. It is seen that the analytic solution obtained via the modified DAC techniques and the weak form solution compare very favorably. Also, the response shown agrees qualitatively with experimental results obtained by Stuetzer (*47*) for PZT-4. The effect of adding artificial damping is clearly evident as the Rayleigh damping completely eliminates the spurious oscillations. Similarly, the modified DAC algorithm and COMSOL numerical results for the response of a quartz disk subjected to a unit step voltage are in excellent agreement (figure 4). In the case of quartz, however, the numerical oscillations due to the solver response to step loadings is more pronounced. While the inclusion of the numerical damping completely eliminates these oscillations, there is a loss of accuracy at the step transitions as a larger value of the damping parameter ν_R was required to fully damp the solver oscillations.

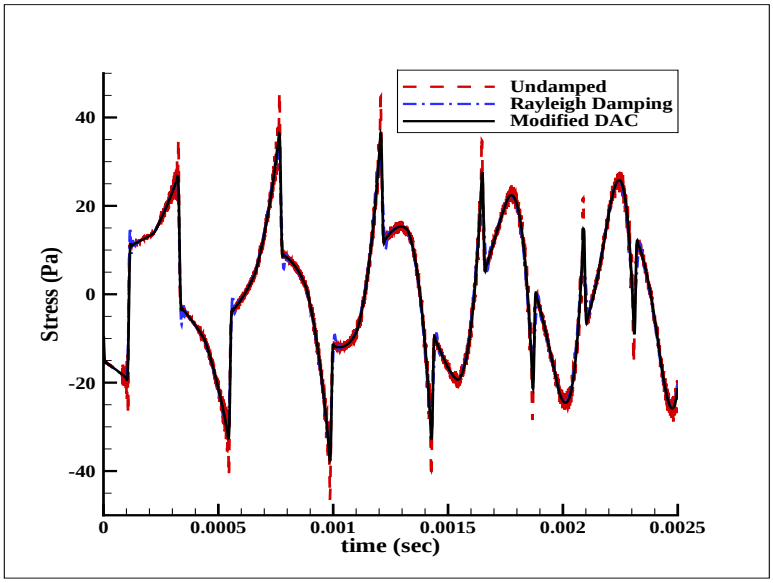

Figure 3. Transient stress history (at x=2.15 mm) in a 4.3-mm-thick PZT-4 disk subjected to a Heaviside step voltage.

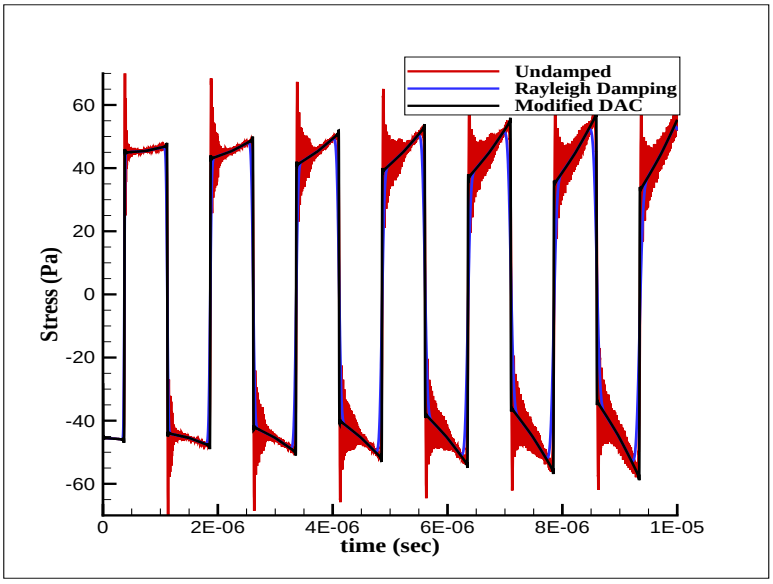

Figure 4. Transient stress history (at x=2.15 mm) in a 4.3-mm-thick quartz disk subjected to a Heaviside step voltage.

The numerical solution was also verified by comparing the resonance response (figure 5). As sinusoidal loading is reasonably smooth, solver oscillations are not induced. It is seen that the numerical and analytical solutions are again in excellent agreement. The effect of the numerical damping is also clearly seen in the reduction in the peak stresses of each loading cycle. Finally, the computed response of a bi-layered piezoelectric media was compared with the Laplace transform solution. The solution was compared at two locations, $l/4$ (figure 6) and $3l/4$ (figure 7), which correspond to the midpoints of the PZT and quartz layers, respectively. It is seen that the response is much more complicated due to internal wave reflections due to the impedance mismatch between the materials. As a consequence, the numerical solution exhibits pronounced ringing effects. It is not possible to reduce this ringing behavior without significant loss of accuracy in the overall response.

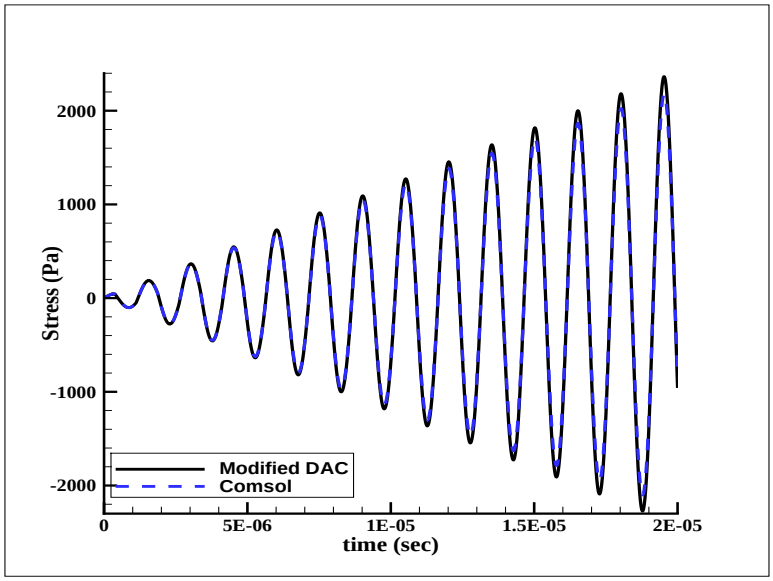

Figure 5. Resonance response (at x=2.15 mm) in a 4.3-mm-thick quartz disk subjected to an harmonic voltage. $\omega = 666$ kHz.

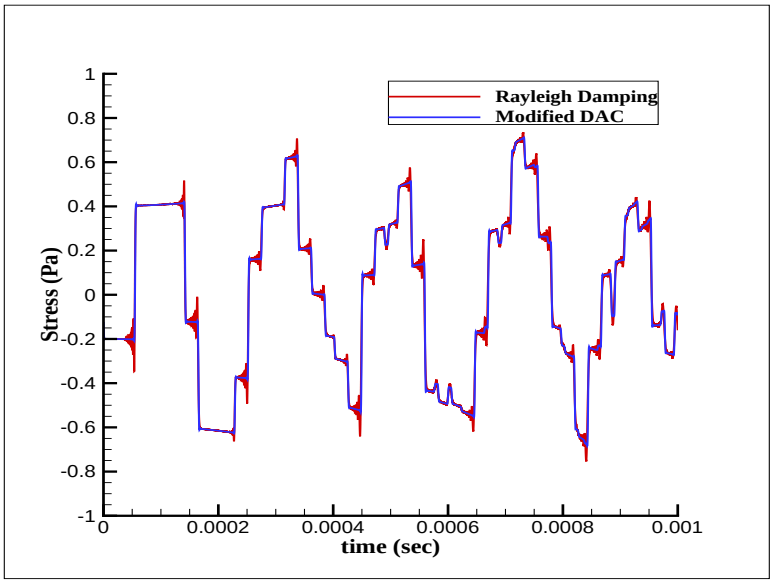

Figure 6. PZT response (x=L/4) in a unit thick PZT-quartz disk subjected to a step voltage.

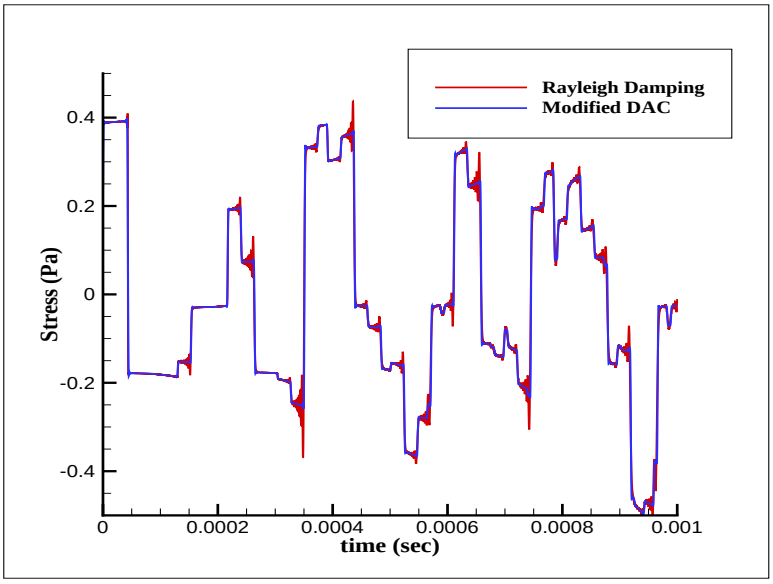

Figure 7. Quartz response (x=3L/4) in a unit thick PZT-quartz disk subjected to a step voltage.

With the numerical solution technique verified by comparison with solutions obtained with the modified DAC algorithm solutions, several cases were studied corresponding to a step pressure load applied at the $x = 0$ endpoint location. The boundary conditions are given the third column of table 2. Results are shown in figure 8. The stress response is normalized in order to highlight the effect of pressure on the response. The 1-GPa linear curve represents the exact solution of the linear piezoelectricity equations to a 1-GPa step pressure. The numerical solution of the nonlinear equations is indistinguishable for this load and is therefore not shown in figure 8. It is seen that the 5-GPa compression result is also almost the same as the 1-GPa linear result. The principal differences are that the normalized peak stress is approximately -2.25 compared with the peak value of -2.0 for the linear result. The wave speed is nearly the same for these loads as indicated by the coincidence of the step changes in the response as the stress wave reflects from the boundaries. Similarly, the 5-GPa tension and 10-GPa compression curves also retain the same basic form as the linear response. However, the wave speed for these two cases, while different from the linear response, are the same. This indicates that the wave speed is not symmetric with respect to the loading level. Furthermore, the wave speed is slower for the 10-GPa compressive load than the linear response. This is in contrast with the linear theory, which predicts that the wave speed should increase with increasing compression load level. An expression for the effective wave speed, c, can be obtained by substituting equations 18, 19, and

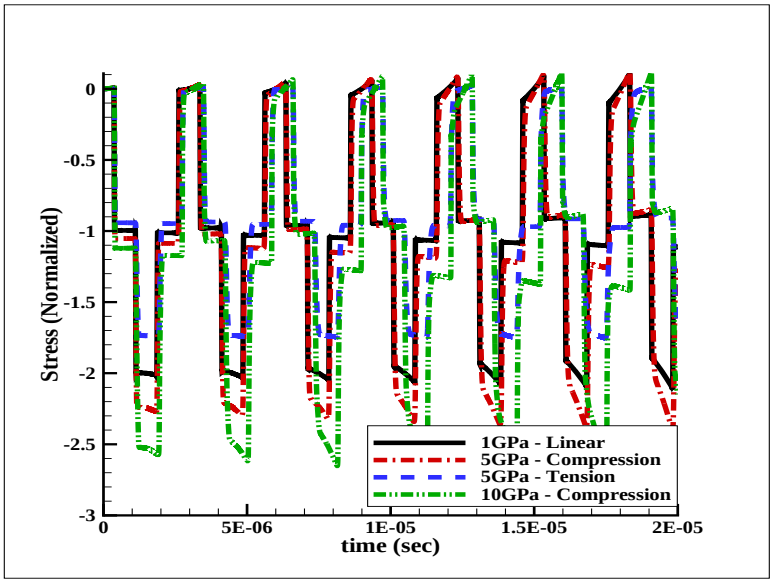

Figure 8. Transient stress histories (at x=2.15 mm) in a 4.3-mm-thick quartz disk subjected to various Heaviside step stress loadings.

21 into the 1-D form of equation of motion, equation 8. This leads to

$$c^2 = \frac{(c^E + C\Gamma - gE)(1 + u_{,Z})^2 + (a\Gamma - eE + \frac{1}{2}C\Gamma^2 - \frac{1}{2}QE^2 - g\Gamma E)}{\rho_0} \quad . \tag{55}$$

If terms arising in equation 55 related to nonlinear affects are dropped, then the expression for c^2 agrees with classical results (*39*). Figure 9 plots c^2 normalized by the linear elastic bar velocity versus the finite strain measure Γ. At $\Gamma = 0$, the wave speed is the same as classical elasticity. For slightly compressive strains, $\Gamma < -2.67\%$, the wave speed increases. However, for higher strain levels, the wave speed decreases. Also, for large finite strains, in either compression or tension, the wave speed is imaginary, which could represent the transition to standing waves. Whether this is correct or simply represents a constraint on the range of validity of the theory is currently being investigated.

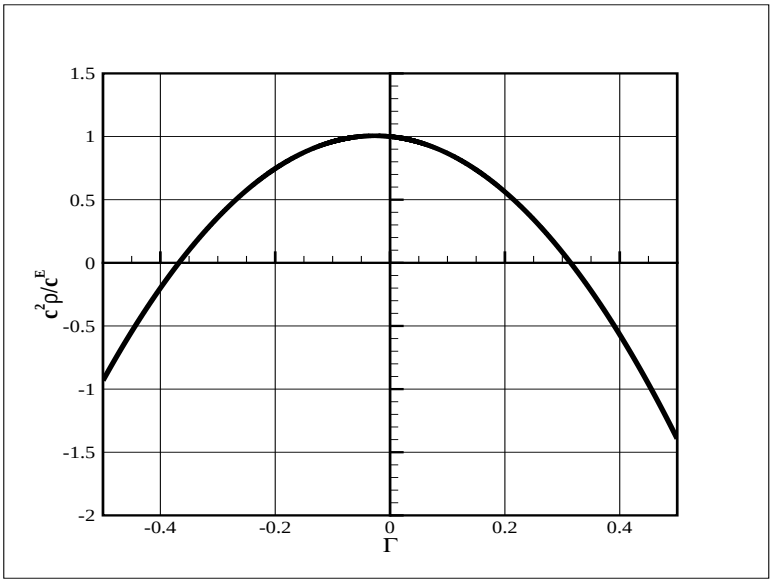

Figure 9. Normalized wave speed squared $c^2\rho/c^E$ vs. finite strain Γ.

7. Conclusions

A second-order theory for the behavior of piezoelectric materials has been presented. It has been shown that the presented theory reduces to the same results as linear piezoelectricity for small strains. The effects of the nonlinear terms have been shown by computing the response of quartz to various levels of pressure, which are realistic for shock loading. In these cases, the theory predicts that for large enough compressive or tensile pressures that the wave speed will decrease. This is in contrast to linear piezoelectricity where the wave speed always increases with increasing compressive stresses. Finally, the second-order theory predicts that governing equations will change behavior at large absolute values of the finite strain. Whether this represents a real phenomena or is simply a restriction on the range of applicability of the theory is currently being investigated.

8. References

1. Lippmann, H.G. Sur le principe de la conversation de l'electricite ou second principe de la theorie des phenomenes electriques. *Comptes Rendes Acad. Sci.* **1881**, *92*, 1049.
2. Shaul K. The Discovery of the Piezoelectric Effect. *Arch. Hist. Exact Sci.* **2003**, *57*, 61–91.
3. Cady W. *Piezoelectricity: An Introduction to the Theory and Applications of Electromechanical Phenomena in Crystals*; Dover Publications: New York, 1964.
4. Kolpakov J.E.; Zhilin P.A., Generalized Continuum and Linear Theory of Piezoelectric Materials. Proceedings of the XXIX Summer School - Conference "Advanced Problems in Mechanics", St. Petersburg, Russia **2002**, 364–375.
5. Tadmor E.B.; Kósa G. Electromechanical Coupling Correction for Piezoelectric Layered Beams. *J. Microelectromechanical Systems* **2003**, *12*, 899–906.
6. Ossadzow-David C.; Touratier M. A multilayered piezoeletric shell theory. *Composites Science and Technology* **2004**, *64*, 2121–2137.
7. Dai, H.L.; Wang, X. Thermo-electro-elastic transient responses in piezoelectric hollow structures. *Int. J. Solids and Structures* **2005**, *42*, 1151–1171.
8. Chen, T. Further correspondences between plane piezoelectricity and generalized plane strain in elasticity. *Proc. R. Soc. Lond.* **1971,** *A454*, 873–884.
9. Chizhikov, S.; Sorokin N.; Petrakov, V. The elastoelectric effect in the non-centrosymmetric crystals. *Ferroelectric* **1982**, *41*, 9–25.
10. Maugin, G. *Continuum Mechanics of Electromagnetic Solids*; North-Holland, 1988.
11. Ashida, F.; Tauchert, T. An inverse problem for determination of transient surface temperature from piezoelectric sensor measurement. *J. Appl. Mech.* **1998**, *65*, 367–373.
12. Chandrasekharaiah, D. A generalized linear thermo-elasticity theory for piezoelectric media. *Acta Mech.* **1998**, *71*, 39–49.
13. Nelson, D. Theory of nonlinear electroacoustics of dielectric piezoelectric crystals. *J. Acoust. Soc. Am.* **1978**, *63*, 1738–1748.

14. Toupin, R. A dynamical theory of elastic dielectrics. *Int. J. Eng. Sci.* **1983**, *21*, 101–126.

15. Tiersten, H. Electroelastic interactions and the piezoelectric equations. *J. Acoust. Soc. Am.* **1981**, *70*, 1567–1576.

16. Tiersten, H. On the Nonlinear Equations of Thermoelectroelasticity. *Int. J. Engineering Sci.* **1971**, *9*, 587–604.

17. Norwood, D.; Shuart, M.; Herakovich, C. Geometrically nonlinear analysis of interlaminar stresses in unsymmetrically laminate plate subject to inplane mechanical loading. *Proceeding of the AIAA/ASME /ASCE/AHS/ACS 32nd Structures, Structural Dynamics and Materials Conference*, Washington DC, 1991, 938–955.

18. Kulkarni G.; Hanagud, S.V. Modeling issues in the vibration control with piezoceramic actuators. *Smart Struct. Mater.*, **1991**, *24*, 7–17.

19. Pai, P.; Nayfeh, A.; Oh, K. A nonlinear theory of laminated piezoelectric plates. *Proceeding of the 33rd AIAA/ASME/ASCE/AHS/ASC Structures, Structural Dynamics and Materials Conference* Washington, DC **1982**, 577–585.

20. Joshi, S. Nonlinear constitutive relations for piezoceramic materials. *Smart. Mater. Struct* **1992**, *1*, 80–83.

21. Tiersten, H. Electroelastic equations for electroded thin plates subjected to large driving voltages. *J. Appl. Phys.* **1993**, *74*, 3389–3393.

22. Patel, M.S.; Yong, Y.; Tanaka, M. Drive level dependency in quartz resonators. *Int. J. Solids Struct.* **2009**, *46* (9), 1856–1871.

23. Yang, J.; Batra, R. A second-order theory for piezoelectric materials. *J. Acoust. Soc. Am.* **1995**, *97*, 280–288.

24. Feng, W.; Gazonas, G.; Hopkins, D.; Pan, E. A second-order theory for piezoelectricity with 6mm and m3 crystal classes. *Smart. Mater. Struct* **2011**, *20*, 045011.

25. Kiral, E.; Eringen, A. *Constitutive equations of nonlinear electromagnetic-elastic crystals*; Springer-Verlag, 1990.

26. Malvern, L. *Introduction to the Mechanics of Continuous Media*; Prentice-Hall, Inc 1969.

27. Pao, Y. Electromagnetic forces in deformable continua. *Mechanics Today vol IV*, **1978**, Pergamon Press, 209–306.

28. Lax, M.; Nelson, D. Maxwell equations in material form. *Physical Review B* **1976** *13* (4), 1777–1784.

29. Dorfmann, A.R.; Odgen, R.W. Nonlinear electroelasticity. *Acta Mechanica* **2000**, *174* (3-4), 167–183.

30. Clayton, J. A non-linear model for elastic dielectric crystals with mobile vacancies. *Int. Jour. of Non-Lin Mech.* **2009**, *44* (6), 675–688.

31. Yang, J.S.; Batra, R.C. A theory of electroded thin thermopiezoelectric plates subject to large driving voltages. *J. Appl. Phys.* **1994**, *76* (9), 5411–5417.

32. Eringen, C. *Mechanics of Continua*; Robert E. Krieger, 1989.

33. Strang, G. *Introduction to Applied Mathematics*; Wellesley-Cambridge Press, 1986.

34. Zielinski, T. Fundamentals of multiphysics modelling of piezo-poro-elastic structures. *Arch. Mech.* **2010**, *62* (5), 343–378.

35. Feng, W.; Pan, E.; Wang, X.; Gazonas, G. A second-order theory for magnetoelectrostatic materials with transverse isotropy. *Smart Mater Struct* **2009**, *18*, 025001.

36. *COMSOL Multiphysics User's Guide*; COMSOL AB, 2008.

37. Piche, R. Numerical Experiments with the Modified Rosenbrock Algorithm for Structural Dynamics. Report 17, Tampere, 1995.

38. Hughes, T. *The Finite Element Method: Linear Static and Dynamic Finite Element Analysis*; Prentice-Hall, 1987.

39. Lysne, P. One-Dimensional Theory of Polarization by Shock Waves: Application to Quartz Gauges. *J Appl. Phys* **1972**, *43* (2), 425–431.

40. Crump, K. Numerical inversion of Laplace transforms using a Fourier series approximation. *Journal of the ACM* **1976**, *23* (1), 89–96.

41. Tarumi, R.; Nakamura, K.; Ogi, H.; Hirao, M. Complete set of elastic and piezoelectric coefficients of α-quartz at low temperatures. *J. App. Phys.* **2007**, 102 (11), 113508.

42. Davison, L.; Graham, R. Shock Compression of Solids. *Physics Reports: Review Section of Physics Letters* **1979**, *55* (4), 255–379.

43. Laverty, R.; Gazonas, G. An improvement to the Fourier series method for inversion of Laplace transforms applied to elastic and viscoelastic waves. *Int. J. Comp. Meth.* **2006**, *3* (1), 57–69.

44. Chen, P.;, Davison, L.; McCarthy, M.F. Electrical responses of nonlinear piezoelectric materials ot plane waves of uniaxial strain. *J. Appl. Phys.* **1976**, *47* (11), 4759–4764.

45. Yang, J. Piezoelectromagnetic Waves in a Ceramic Plate. *IEEE Transactions on Ultrasonics, Ferroelectrics, and Frequency Control* **2004**, *51* (8), 1035–1039.

46. Redwood, M. Transient Performance of a Piezoelectric Transducer. *J. Acoust. Soc. Am.* **1961**, *33* (4), 527–536.

47. Stuetzer O. Multiple Reflections in a Free Piezoelectric Plate. *J. Acoust. Soc. Am.* **1964**, *42*, 502–508.

48. *IEEE Standard on Piezoelectricity* (IEEE Standard 176-1987), The Institute of Electrical and Electronics Engineers, 345 East 47th St, New York, NY 10017, 1987.

Appendix A. Bi-material Solution

The Laplace transform solutions for the stresses in each layer of the bi-material slab are given by

$$\sigma_1(x,s) = -\frac{2\varepsilon_1\varepsilon_2 M_1 M_2 V_0 A_7 e^{-\frac{sx}{c_1}} \left(c_2 M_1 \left(h_1 A_1 A_2 A_8 - h_2 e^{\frac{s}{2c_1}} {A_6}^2 A_9\right) - c_1 h_1 M_2 A_3 A_{10}\right)}{A_{15} + A_{16} - A_{17} + A_{18}} \tag{A-1}$$

$$\sigma_2(x,s) = \frac{2\varepsilon_1\varepsilon_2 M_1 M_2 V_0 A_{11} e^{-\frac{s(x+1)}{c_2}} \left(c_2 h_2 M_1 e^{\frac{s}{c_2}} A_4 A_{12} + c_1 M_2 e^{\frac{s}{2c_2}} \left(h_1 {A_2}^2 A_{13} - h_2 A_5 A_6 A_{14}\right)\right)}{A_{15} + A_{16} - A_{17} + A_{18}} \tag{A-2}$$

where

$$
\begin{aligned}
A_1 &= \left(e^{\frac{s}{c_2}} + 1\right) \\
A_2 &= \left(e^{\frac{s}{2c_1}} - 1\right) \\
A_3 &= \left(e^{\frac{s}{c_2}} - 1\right) \\
A_4 &= \left(e^{\frac{s}{c_1}} - 1\right) \\
A_5 &= \left(e^{\frac{s}{c_1}} + 1\right) \\
A_6 &= \left(e^{\frac{s}{2c_2}} - 1\right) \\
A_7 &= \left(e^{\frac{sx}{c_1}} - 1\right) \\
A_8 &= \left(e^{\frac{sx}{c_1}} - e^{\frac{s}{2c_1}}\right) \\
A_9 &= \left(e^{\frac{sx}{c_1}} + 1\right) \\
A_{10} &= \left(e^{\frac{s}{c_1}} - e^{\frac{sx}{c_1}}\right) \\
A_{11} &= \left(e^{\frac{s}{c_2}} - e^{\frac{sx}{c_2}}\right) \\
A_{12} &= \left(e^{\frac{sx}{c_2}} - 1\right) \\
A_{13} &= \left(e^{\frac{sx}{c_2}} + e^{\frac{s}{c_2}}\right) \\
A_{14} &= \left(e^{\frac{s}{2c_2}} - e^{\frac{sx}{c_2}}\right) \\
A_{15} &= 2c_2^2\varepsilon_1\varepsilon_2 h_2^2 M_1^2 A_3 A_4 \\
A_{16} &= c_2 M_2 M_1 \left(4c_1\varepsilon_1\varepsilon_2 \left(h_2^2 A_5 {A_6}^2 - h_1 h_2 {A_2}^2 {A_6}^2 + h_1^2 A_1 {A_2}^2\right)\right) \\
A_{17} &= \left(\varepsilon_1 + \varepsilon_2\right) M_1 s A_1 A_4) \\
A_{18} &= c_1 M_2^2 A_3 \left(2c_1\varepsilon_1\varepsilon_2 h_1^2 A_4 - \left(\varepsilon_1 + \varepsilon_2\right) M_1 s A_5\right)
\end{aligned}
\tag{A-3}
$$

Appendix B. Linear Piezoelectric Constitutive Relations

The following forms of linear piezoelectric constitutive relationships are given by the *IEEE Standard on Peizoelectricity* (*48*). There are four standard forms of the linear piezoelectric constitutive laws. Written in tensor notation, these forms are

$$\begin{aligned} T_{ij} &= c^E_{ijkl} S_{kl} - e_{kij} E_k \\ D_i &= e_{ikl} S_{kl} + \epsilon^S_{ik} E_k \end{aligned} \tag{B-1}$$

$$\begin{aligned} T_{ij} &= c^D_{ijkl} S_{kl} - h_{kij} D_k \\ E_i &= -h_{ikl} S_{kl} + \beta^S_{ik} D_k \end{aligned} \tag{B-2}$$

$$\begin{aligned} S_{ij} &= s^E_{ijkl} T_{kl} - d_{kij} E_k \\ D_i &= d_{ikl} T_{kl} + \epsilon^T_{ik} E_k \end{aligned} \tag{B-3}$$

$$\begin{aligned} S_{ij} &= s^D_{ijkl} T_{kl} + g_{kij} D_k \\ E_i &= -g_{ikl} T_{kl} + \beta^T_{ik} D_k \end{aligned} \tag{B-4}$$

Using Voigt notation, the above relationships can be written as

$$\begin{aligned} T_p &= c^E_{pq} S_q - e_{kp} E_k \\ D_i &= e_{iq} S_q + \epsilon^S_{ik} E_k \end{aligned} \tag{B-5}$$

$$\begin{aligned} T_p &= c^D_{pq} S_q - h_{kp} D_k \\ E_i &= -h_{iq} S_q + \beta^S_{ik} D_k \end{aligned} \tag{B-6}$$

$$\begin{aligned} S_p &= s^E_{pq} T_q - d_{kp} E_k \\ D_i &= d_{iq} T_q + \epsilon^T_{ik} E_k \end{aligned} \tag{B-7}$$

$$\begin{aligned} S_p &= s^D_{pq} T_q + g_{kp} D_k \\ E_i &= -g_{iq} T_q + \beta^T_{ik} D_k \end{aligned} \tag{B-8}$$

where the ranges on the subscripts are $i, k = 1, 2, 3$ and $p, q = 1, 2, 3, 4, 5, 6$.

The relationship between the coefficients is found using equations B-5–B-8. In our results, the relationship that is required is between the coefficients of the Stress-Charge form, equation B-5,

and the Stress-Voltage form, equation B-6.

$$\begin{aligned} c_{pq}^{D} &= c_{pq}^{E} + e_{kp} h_{kp} \\ e_{kp} &= h_{ip} \epsilon_{ki} \end{aligned} \tag{B-9}$$

In one dimension, this reduces to

$$\begin{aligned} c^{D} &= c^{E} + eh \\ h &= \tfrac{e}{\epsilon} \end{aligned} \tag{B-10}$$

NO. OF COPIES	ORGANIZATION
1 (PDF ONLY)	DEFENSE TECHNICAL INFORMATION CTR DTIC OCA 8725 JOHN J KINGMAN RD STE 0944 FORT BELVOIR VA 22060-6218
1	DIRECTOR US ARMY RESEARCH LAB IMNE ALC HRR 2800 POWDER MILL RD ADELPHI MD 20783-1197
1	DIRECTOR US ARMY RESEARCH LAB RDRL CIO LL 2800 POWDER MILL RD ADELPHI MD 20783-1197
1	DIRECTOR US ARMY RESEARCH LAB RDRL CIO MT 2800 POWDER MILL RD ADELPHI MD 20783-1197
1	DIRECTOR US ARMY RESEARCH LAB RDRL D 2800 POWDER MILL RD ADELPHI MD 20783-1197

NO. OF COPIES	ORGANIZATION
2	NSF S MCKNIGHT G PAULINO 4201 WILSON BLVD, STE 545 ARLINGTON, VA, 22230-0002
2	DARPA W COBLENZ J GOLDWASSER 3701 N FAIRFAX DR ARLINGTON VA 22203-1714
1	DIRECTOR US ARMY ARDEC AMSRD AAR AEE W E BAKER BLDG 3022 PICATINNY ARSENAL NJ 07806-5000
2	US ARMY TARDEC AMSTRA TR R MS 263 K BISHNOI D TEMPLETON MS 263 WARREN MI 48397-5000
CD	COMMANDER US ARMY RSRCH OFC RDRL ROI M J LAVERY PO BOX 12211 RESEARCH TRIANGLE PARK NC 27709-2211
1	COMMANDER US ARMY RSRCH OFC RDRL ROE M D STEPP PO BOX 12211 RESEARCH TRIANGLE PARK NC 27709-2211
6	NAVAL RESEARCH LAB E R FRANCHI CODE 7100 M H ORR CODE 7120 J A BUCARO CODE 7130 G J ORRIS 7140 J S PERKINS CODE 7140 S A CHIN BING CODE 7180 4555 OVERLOOK AVE SW WASHINGTON DC 20375

NO. OF COPIES	ORGANIZATION
1	DTRA M GILTRUD 8725 JOHN J KINGMAN RD FORT BELVOIR VA 22060
1	ERDC US ARMY CORPS OF ENGINEERS USACEGSL P PAPADOS 7701 TELEGRAPH RD ALEXANDRIA VA 22315
1	AFOSR/NL 875 NORTH RANDOLPH ST SUITE 325, RM 3112 F FAHROO ARLINGTON VA 22203
1	CLEMSON UNIV DEPT MECH ENGINEERS M GRUJICIC 241 ENGRG INNOVATION BLDG CLEMSON SC 29634-0921
1	UNIV OF CALIFORNIA CTR OF EXCELLENCE FOR ADV MATLS S NEMAT NASSER SAN DIEGO CA 92093-0416
3	DIRECTOR LANL P MAUDLIN A ZUREK F ADDESSIO PO BOX 1663 LOS ALAMOS NM 87545
7	DIRECTOR SANDIA NATL LABS J BISHOP MS 0346 E S HERTEL JR MS 0382 W REINHART MS 1181 T VOGLER MS 1181 L CHHABILDAS MS 1811 M FURNISH MS 1168 M KIPP MS 0378 PO BOX 5800 ALBUQUERQUE NM 87185-0307

NO. OF COPIES	ORGANIZATION
1	DIRECTOR LLNL M J MURPHY PO BOX 808 LIVERMORE CA 94550
3	CALTECH M ORTIZ MS 105 50 G RAVICHANDRAN T J AHRENS MS 252 21 1201 E CALIFORNIA BLVD PASADENA CA 91125
5	SOUTHWEST RSRCH INST C ANDERSON K DANNEMANN T HOLMQUIST G JOHNSON J WALKER PO DRAWER 28510 SAN ANTONIO TX 78284
1	TEXAS A&M UNIV DEPT OF MATHEMATICS J WALTON COLLEGE STATION TX 77843
1	UNIVERSITY OF MISSISSIPPI DEPT OF MECH ENGRG A M RAJENDRAN 201-B CARRIER HALL UNIVERSITY, MS 38677
2	SRI INTERNATIONAL D CURRAN D SHOCKEY 333 RAVENSWOOD AVE MENLO PARK CA 94025
1	VIRGINIA POLYTECHNIC INST COLLEGE OF ENGRG R BATRA BLACKSBURG VA 24061-0219
7	UNIV OF NEBRASKA DEPT OF ENGRG MECH F BOBARU Y DZENIS G GOGOS M NEGAHBAN R FENG J TURNER Z ZHANG LINCOLN NE 68588

NO. OF COPIES	ORGANIZATION
1	JOHNS HOPKINS UNIV DEPT OF MECH ENGRG K T RAMESH LATROBE 122 BALTIMORE MD 21218
1	WORCESTER POLYTECHNIC INST MATHEMATICAL SCI K LURIE WORCESTER MA 01609
4	UNIV OF UTAH DEPT OF MATH A CHERKAEV E CHERKAEV E S FOLIAS R BRANNON SALT LAKE CITY UT 84112
1	PENN STATE UNIV DEPT OF ENGRG SCI & MECH F COSTANZO UNIVERSITY PARK PA 168023
4	UNIV OF DELAWARE DEPT OF MECH ENGRG T BUCHANAN T W CHOU A KARLSSON M SANTARE 126 SPENCER LAB NEWARK DE 19716
1	UNIV OF DELAWARE CTR FOR COMPST MATRLS J GILLESPIE NEWARK DE 19716
1	COMPUTATIONAL MECH CONSULTANTS J A ZUKAS PO BOX 11314 BALTIMORE MD 21239-0314
1	LOUISIANA STATE UNIV R LIPTON 304 LOCKETT HALL BATON ROUGE LA 70803-4918
1	INST OF ADVANCED TECH UNIV OF TX AUSTIN S BLESS 3925 W BRAKER LN STE 400 AUSTIN TX 78759-5316

NO. OF COPIES ORGANIZATION

1 APPLIED RSCH ASSOCIATES
D E GRADY
4300 SAN MATEO BLVD NE
STE A220
ALBUQUERQUE NM 87110

1 INTERNATIONAL RSRCH
ASSOC INC
D L ORPHAL
4450 BLACK AVE
PLEASANTON CA 94566

2 WASHINGTON ST UNIV
INST OF SHOCK PHYSICS
Y M GUPTA
J ASAY
PULLMAN WA 99164-2814

1 NORTHWESTERN UNIV
DEPT OF CIVIL & ENVIRON ENGRG
Z BAZANT
2145 SHERIDAN RD A135
EVANSTON IL 60208-3109

1 UNIV OF DAYTON
RSRCH INST
N S BRAR
300 COLLEGE PARK
MS SPC 1911
DAYTON OH 45469

2 TEXAS A&M UNIV
DEPT OF GEOPHYSICS MS 3115
F CHESTER
T GANGI
COLLEGE STATION TX 778431

1 UNIV OF SAN DIEGO
DEPT OF MATH & CMPTR SCI
A VELO
5998 ALCALA PARK
SAN DIEGO CA 92110

1 NATIONAL INST OF
STANDARDS & TECHLGY
BLDG & FIRE RSRCH LAB
J MAIN
100 BUREAU DR MS 8611
GAITHERSBURG MD 20899-8611

NO. OF COPIES ORGANIZATION

1 MIT
DEPT ARNTCS ASTRNTCS
R RADOVITZKY
77 MASSACHUSETTS AVE
CAMBRIDGE MA 02139

1 UNIV OF DELAWARE
DEPT ELECTRICAL & CMPTR ENGRG
D WEILE
NEWARK DE 19716

1 T W WRIGHT
4906 WILMSLOW RD
BALTIMORE MD 21210

1 UNIV OF TEXAS-PAN AMERICAN
COLLEGE OF ENGRG
& COMPUTER SCI
D H ALLEN
1201 WEST UNIVERSITY DR
EDINBURG, TX 78539-2999

3 RDRL D
C CHABALOWSKI
J CHANG
R SKAGGS
BLDG 205
2800 POWDER MILL RD
ADELPHI MD 20783-1197

ABERDEEN PROVING GROUND

85 DIR USARL
RDRL CIH C
J CAZAMIAS
P CHUNG
D GROVE
J KNAP
RDRL WM
B FORCH
S KARNA
J MCCAULEY
P PLOSTINS
M ZOLTOSKI
RDRL WML
D LYONS
J NEWILL
RDRL WML B
I BATYREV
S IZVYEKOV
B RICE
N WEINGARTEN
RDRL WML D

NO. OF COPIES	ORGANIZATION
	P CONROY
	M NUSCA
	RDRL WML G
	M BERMAN
	W DRYSDALE
	RDRL WML H
	D SCHEFFLER
	S SCHRAML
	B SCHUSTER
	RDRL WMM
	J BEATTY
	R DOWDING
	J ZABINSKI
	RDRL WMM A
	J TZENG
	E WETZEL
	RDRL WMM B
	T BOGETTI
	B CHEESEMAN
	C FOUNTZOULAS
	G GAZONAS
	D HOPKINS
	P MOY
	B POWERS
	C RANDOW
	T SANO
	M VANLANDINGHAM
	R WILDMAN
	C F YEN
	RDRL WMM C
	J LA SCALA
	RDRL WMM D
	E CHIN
	K CHO
	RDRL WMM E
	J ADAMS
	M COLE
	T JESSEN
	J LASALVIA
	P PATEL
	J SANDS
	J SINGH
	RDRL WMM F
	L KECSKES
	H MAUPIN
	RDRL WML G
	J ANDZELM
	A RAWLETT
	RDRL WMP
	P BAKER
	S SCHOENFELD

NO. OF COPIES	ORGANIZATION
	RDRL WMP B
	R BECKER
	S BILYK
	D CASEM
	J CLAYTON
	M GREENFIELD
	C HOPPEL
	R KRAFT
	B LEAVY
	M RAFTENBERG
	S SATAPATHY
	M SCHEIDLER
	T WEERASOORIYA
	RDRL WMP C
	T BJERKE
	S SEGLETES
	RDRL WMP D
	R DONEY
	D KLEPONIS
	J RUNYEON
	B SCOTT
	H MEYER
	RDRL WMP E
	M BURKINS
	B LOVE
	RDRL WMP F
	M CHOWDHURY
	A FRYDMAN
	N GNIAZDOWSKI
	R GUPTA
	RDRL WMP G
	N ELDREDGE
	D KOOKER
	S KUKUCK
	G R PEHRSON

INTENTIONALLY LEFT BLANK.